THE FORCED KORTEWEG–DE VRIES EQUATION AS A MODEL FOR WAVES GENERATED BY TOPOGRAPHY

PAUL A. MILEWSKI *

Abstract. This is a brief survey article discussing simple yet very rich models for free surface flows over topographical features. We consider the most interesting case where the flow is near critical (the Froude number is near 1). We derive Korteweg-de Vries and Burgers' equations, and consider both steady configurations and time-dependent numerical solutions. The topography is taken to be either a localized bump or hole or a more extended plateau or depression. The calculations involving extended topography are new and in some cases show surprisingly complex dynamics.

1. Introduction. In this paper we consider a model to describe the evolution of the free-surface when a fluid flows over an obstacle. We shall see that the free surface dynamics will depend on the speed of the flow and the characteristics of the obstacle. We shall focus on the *resonant* case, where the most interesting and largest free-surface response occurs. The problem of flow over an obstacle has applications in many physical situations, from the flow of water over rocks to atmospheric and oceanic stratified flows encountering topographic obstacles [1]. (Equations similar to those we study here can be derived in the stratified flow case.) In addition, the equations we discuss can also be obtained when one considers a pressure distribution moving over a free surface and generating waves. Physical examples of this are models of ship waves, and of ocean waves generated by storms.

Figure 1.1 shows the physical problem we are considering. We shall discuss only the one- dimensional free surface case and derive an approximate governing equation for the free surface evolution η over a topography h:

$$\eta_\tau + f\eta_\xi - \frac{1}{6}\eta_{\xi\xi\xi} - \frac{3}{2}\eta\eta_\xi = \frac{1}{2}h_\xi. \tag{1.1}$$

This equation is known as the forced Korteweg-de Vries (KdV) equation (see [12], [7], [4] for early references) and includes the effects of nonlinearity, dispersion, topography and flow when these effects are comparable to each other in importance. The unforced equation ($h = 0$) has been extensively studied both for its mathematical properties (integrability and inverse scattering theory was first studied on the KdV equation) and its approximation to free nonlinear waves. At smaller scales, when surface tension is comparable to gravity, one can obtain similar models with a fifth derivative term (see [9]).

The important parameter in this problem is the Froude number

$$F = \frac{U}{\sqrt{gH}},$$

which is the ratio of the flow speed to the linear shallow water wave speed. The parameter f appearing in (1.1) is proportional to $F - 1$. Flows that are faster than the linear wave speed ($f > 0$) are called supercritical and $f < 0$ is called subcritical.

We shall consider three main variations on (1.1): 1. The case where the free surface is steady. 2. The "shallow water" limit where the equation is nondispersive (the $\eta_{\xi\xi\xi}$ term is ommitted). 3. The full equation (1.1). These cases will be studied

*Department of Mathematics, University of Wisconsin, 480 Lincoln Dr., Madison, WI 53706 (milewski@math.wisc.edu). Paul Milewski is partially supported by NSF-DMS

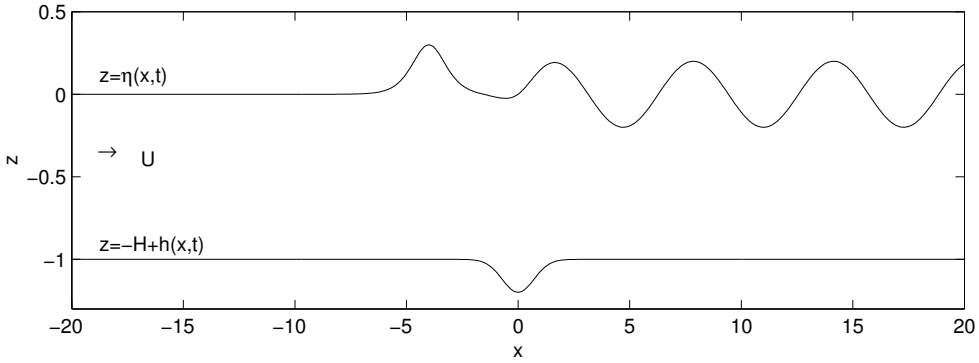

FIG. 1.1. *Sketch of physical problem.*

for two main types of topography: localized bumps and holes, and extended plateaus or depressions. Previous studies of this problem have focussed only on the flow over a localized bumps, not on holes or extended topography. This is possibly due to the fact that when water flows over a hole there is a stronger possibility of flow separation and recirculation in the hole, effects that are beyond the present theory. However, if the hole is not too abrupt (certainly in the case of an extended depression), the current model is still valid. Wherever possible we construct exact solutions, but for most cases our solutions are numerical.

2. The forced Korteweg-de Vries equation. For the purposes of the derivation, instead of considering a uniform flow over a fixed topographic obstacle, it is convenient to view the obstacle moving at a fixed speed U under a fluid at rest. Then, using the typical wavelength L as the horizontal length scale, the far field depth H as the vertical length scale and a as the scale for typical free surface displacements and the topography, we define the nonlinearity parameter $\epsilon = a/H$ and the long wave (or dispersive) parameter as $\mu = H/L$. These will be the small parameters on which our asymptotic theory is based. The case $\mu = 0$ is usually called the *shallow water* limit whereas μ small but finite is called the *long wave* limit. Using $a\mu\sqrt{gH}$ as the velocity potential scale, $L/\sqrt{gH}$ as the time scale, the dimensionless equations for an irrotational fluid with a free surface can be written in terms of the velocity potential $\phi(x, z, t)$, the bottom boundary $-H + h(x + Ut)$, and the free surface displacement $\eta(x, t)$ as

$$\mu^2\phi_{xx} + \phi_{zz} = 0, \quad -1 + \epsilon h(x + Ft) < z < \epsilon\eta(x, t), \tag{2.1}$$

$$\mu^2(Fh_x + \epsilon\phi_x h_x) - \phi_z = 0, \quad z = -1 + \epsilon h(x + Ft), \tag{2.2}$$

$$\eta_t + \epsilon\eta_x\phi_x - \frac{1}{\mu^2}\phi_z = 0, \quad z = \epsilon\eta, \tag{2.3}$$

$$\phi_t + \epsilon\left(\frac{\phi_x^2}{2} + \frac{1}{\mu^2}\frac{\phi_z^2}{2}\right) + \eta = 0, \quad z = \epsilon\eta. \tag{2.4}$$

Here, $F = U/\sqrt{gH}$ is the Froude number. Laplace's equation (2.1) follows from the incompressibility of the fluid, (2.2) is the condition of no fluid flux through the

bottom, (2.3) is the statement that η is carried with the flow, and (2.4) is Bernoulli's equation stating that the pressure at the free surface is a constant (taken as zero). Expanding the two surface boundary conditions (2.4,2.3) about $z = 0$ and eliminating η leads to a single boundary condition in ϕ at $z = 0$ correct to $\mathrm{O}(\epsilon)$:

$$\phi_{tt} + \frac{1}{\mu^2}\phi_z + \epsilon\left[\frac{1}{2}\left(\phi_x^2 + \frac{1}{\mu^2}\phi_z^2\right)_t - (\phi_t\phi_{tz})_t + (\phi_t\phi_x)_x\right] = 0, \quad z = 0. \tag{2.5}$$

Next, we write the solution to Laplace's equation (2.1) in the vertical as

$$\phi(x, z, t) = \cos\left[\mu(z+1)\partial_x\right]\Phi(x,t) + \mu\sin\left[\mu(z+1)\partial_x\right]\partial_x^{-1}\Psi(x,t). \tag{2.6}$$

The trigonometric functions appearing above should be thought as representing their Taylor expansions. Note that $\Phi = \phi(x, -1, t)$ and that $\Psi = \mu^{-2}\phi_z(x, -1, t)$. The leading order velocity is depth independent and is given by Φ_x and the free surface displacement can be recovered from (2.4) and (2.6) as

$$\eta \approx -\phi_t \approx -\Phi_t \tag{2.7}$$

We now substitute this solution in the free surface condition (2.5) and the bottom boundary condition (2.2), yielding two equations for our unknowns Φ and Ψ, respectively:

$$\begin{aligned}\Phi_{tt} - \Phi_{xx} + \Psi + \mu^2\left[\frac{1}{6}\Phi_{xxxx} - \frac{1}{2}\Phi_{xxtt} + \Psi_{tt} - \frac{1}{2}\Psi_{xx}\right] \\ + \epsilon\left[\frac{1}{2}(\Phi_x^2)_t + (\Phi_t\Phi_x)_x\right] = 0\end{aligned} \tag{2.8}$$

$$\mu^2 F h_x + \mu\sin\left[\mu\epsilon h\partial_x\right]\Phi_x - \mu^2\cos\left[\mu\epsilon h\partial_x\right]\Psi = 0. \tag{2.9}$$

Equation (2.8) has been truncated to $O(\epsilon)$ and $O(\mu^2)$ and a similar truncation on (2.9) yields:

$$Fh_x - \Psi + \epsilon\left[h\Phi_{xx}\right] = 0. \tag{2.10}$$

We first consider the simplest case of free surface dynamics, the linear shallow water case obtained by setting $\epsilon = \mu^2 = 0$ in (2.8,2.10)

$$\Phi_{tt} - \Phi_{xx} = -Fh_x(x + Ft). \tag{2.11}$$

We are interested here in the surface displacements due to the topography so we always consider cases with zero initial data. The particular solution of (2.11) is

$$\Phi = \frac{F}{1 - F^2}\int h(x + Ft)\, dx. \tag{2.12}$$

Therefore, the surface displacement

$$\eta \approx \frac{F^2}{F^2 - 1}h(x + Ft), \tag{2.13}$$

is steady relative to the obstacle and follows the bottom shape for $F > 1$. The homogeneous solution (often called the free waves) travels with speed ± 1 and therefore, for

F not close to ± 1, propagates away from a localized bottom obstacle. The approximation of (2.11) becomes invalid when $F \approx \pm 1$, because the free surface displacement becomes large, and because the free waves may remain over the obstacle for long enough times to be affected by it. In fact, when $F^2 - 1 = O(\epsilon)$, we need to rescale the bottom to size $O(\epsilon^2)$ for the surface displacement to remain $O(\epsilon)$ as required by the expansion. (In obtaining (2.11) the bottom was assumed to be $O(\epsilon)$.) This is called the *resonant* case because a small topography generates a relatively large free-surface response.

There is another physical situation in which there is a possible resonance between the waves and the topography. Bragg scattering occurs when periodic waves scatter over periodic topography. A resonant form of Bragg scattering will take place when the scattered waves are themselves free modes of the system. This limit is modeled by coupled KdV equations in [2].

Now, considering the distinguished limit obtained by balancing the nonlinear, topographic and dispersive effects, we put $\epsilon = \mu^2$, $F = 1 + \epsilon f$, and $h \to \epsilon h$ into (2.8,2.10). These become

$$\Phi_{tt} - \Phi_{xx} + \epsilon \left[\frac{1}{6}\Phi_{xxxx} - \frac{1}{2}\Phi_{xxtt} + \frac{1}{2}(\Phi_x^2)_t + (\Phi_t \Phi_x)_x \right] = -\epsilon h_x(x + t + \epsilon f t). \tag{2.14}$$

We now consider waves traveling only to the left at a speed close to -1. This is because the waves traveling at speeds close to $+1$ will be far from resonant and relatively small. We do this by moving to the frame of the obstacle by setting $\xi = x + (1 + \epsilon f)t$, $\tau = \epsilon t$ and $\eta(\xi, \tau) \equiv -\Phi_\xi$. A final truncation of the equation leads to

$$\eta_\tau + f\eta_\xi - \frac{1}{6}\eta_{\xi\xi\xi} - \frac{3}{2}\eta\eta_\xi = \frac{1}{2}h_\xi(\xi). \tag{2.15}$$

This is the Forced Korteweg de-Vries Equation that we study in the remainder of the paper. It governs the slow dynamics of the free surface shown in Figure 1.1 when the flow velocity U is close to $\sqrt{gH}$. We shall always assume an infinite domain $-\infty < \xi < \infty$ and that $\eta(\xi, 0) = 0$. This corresponds to a quiescent flow which at $t = 0$ is impulsively started over the topography. We will mainly be interested in the behavior after initial transients have propagated away.

The equation (2.15) conserves mass, with:

$$\frac{d}{d\tau}\int_{-\infty}^{\infty} \eta d\xi = 0, \tag{2.16}$$

and the rate of change of momentum is given by the topographical stress:

$$\frac{d}{d\tau}\int_{-\infty}^{\infty} \eta^2 d\xi = \int_{-\infty}^{\infty} \eta h_\xi d\xi = -\int_{-\infty}^{\infty} \eta_\xi h d\xi, \tag{2.17}$$

where the last equality is obtained by integration by parts. In subsequent sections we shall find several types of steady solutions near the localized topography, and they yield different topographical stresses. These are: 1. Localized free surface deflections. These solutions have zero stress, and the topography does no work on the fluid; 2. Hydraulic "falls": monotonic solutions tending to different values up and downstream from the topography. These solutions do add energy to the flow since η_ξ has one sign. 3. Shocks. These solutions also do work on the fluid proportional to the height of the topography under the shock.

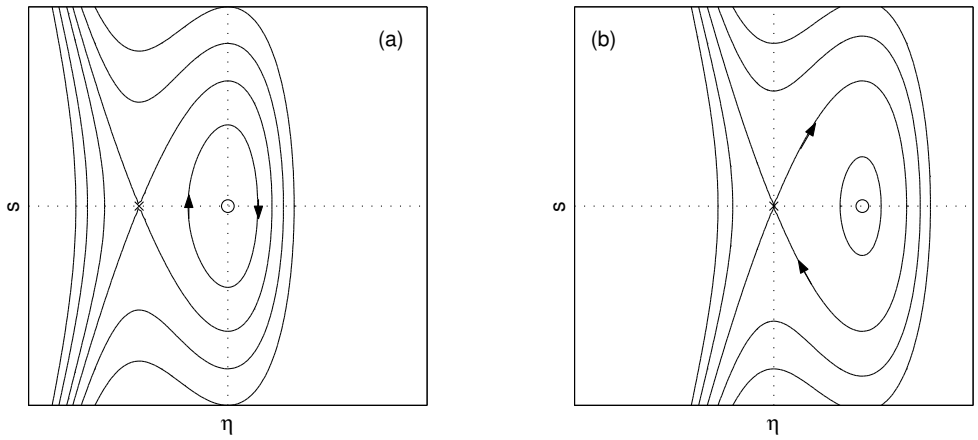

FIG. 3.1. *Phase plane of the unforced problem for $E = 0$. (a) $f < 0$, (b) $f > 0$. Circles indicate centers and crosses indicate saddles.*

For $h = 0$ (2.15) is the well known Korteweg-de Vries equation with solitary wave solutions

$$\eta = A\mathrm{sech}^2(\kappa\xi - c\tau), \qquad A = \frac{4}{3}\kappa^2, \qquad c = f + \frac{1}{2}A. \tag{2.18}$$

The parameter f defines how close the flow is to exact resonance ($F = 1$). In the remainder of the paper we shall consider two main cases with $h \neq 0$: the case when h a highly localized bump or hole, and the case when h corresponds to a long depression or plateau.

3. Localized topography and steady solutions. In this section we study steady solutions of (2.15) when the topography is a localized bump, first with a phase plane analysis and $h = \alpha\delta(\xi)$ (where δ is a Dirac mass), and then with the hydraulic approximation for a smoother bump.

The steady equation from (2.15) is

$$f\eta - \frac{1}{6}\eta_{\xi\xi} - \frac{3}{4}\eta^2 = \frac{1}{2}h - E, \tag{3.1}$$

where E is a constant that enforces zero mean free surface elevation

$$\lim_{L\to\infty} \frac{1}{2L}\int_{-L}^{L} \eta d\xi = 0. \tag{3.2}$$

Thus, we have

$$E = \lim_{L\to\infty} \frac{1}{2L}\int_{-L}^{L} \frac{3}{4}\eta^2 d\xi \geq 0. \tag{3.3}$$

If η tends to zero at both $\xi = \pm\infty$, then $E = 0$. There are physically important steady solutions for which the free surface is constant (but not zero) upstream of the bump and either constant or periodic downstream. In these cases, $E \neq 0$. This state is reached as $t \to \infty$ in (2.15) only if work is continually done by the topography on the fluid (compare (2.17) and (3.3)).

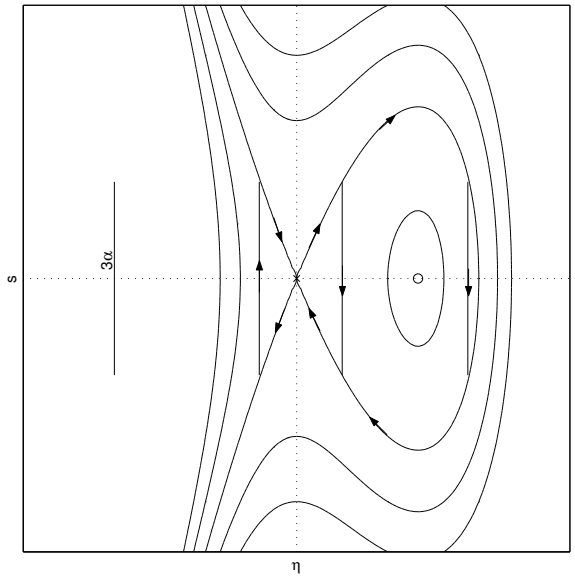

FIG. 3.2. *Solutions to the steady problem for $f > 0$ with Dirac topography $h = \alpha\delta(x)$. The free-surface has a jump in slope of -3α over the bump. There are two solutions shown for $\alpha > 0$ and one for $\alpha < 0$. Other possible solutions are discussed in the text.*

3.1. Flat bottom. For $h = 0$, the solutions η can be described in the phase plane with the equations for $s \equiv \eta_\xi$ and η

$$\begin{aligned} \eta_\xi &= s, \\ s_\xi &= 6f\eta - \frac{9}{2}\eta^2 + 6E. \end{aligned} \tag{3.4}$$

When $E = 0$, the system has, for $f > 0$, a saddle at $\eta = 0$ and a center at $\eta = \frac{4}{3}f$, and, for $f < 0$, a center at $\eta = 0$ and a saddle at $\eta = \frac{4}{3}f$. (There is a transcritical bifurcation at $f = 0$). The system (3.4) is integrable, with the integral curves satisfying

$$\mathcal{H}(\eta, s) = f\eta^2 - \frac{1}{6}s^2 - \frac{1}{2}\eta^3 + 2E\eta = \text{constant}. \tag{3.5}$$

The phase plane for $E = 0$ is shown in Figure 3.1.

The homoclinic orbit for $f > 0$ corresponds to the solitary wave of elevation (2.18), which has zero mean surface elevation. The maximum slope of the solitary wave is $s_{max} = \frac{4\sqrt{2}}{3}f^{3/2}$ and its amplitude is $u_{max} = 2f$. Note that for $f < 0$ the homoclinic orbit has $\lim_{\xi\to\pm\infty}\eta \neq 0$, meaning that the mean surface elevation is no longer zero, and, therefore, that this solution is unphysical. The periodic orbits in Figure 3.1 correspond to nonlinear periodic waves which are also called cnoidal waves from the cn elliptic functions that describe them. These periodic waves also have nonzero mean for the case $E = 0$, but we shall see that they are important and will require us to consider $E \neq 0$.

3.2. Dirac bump. We consider now the case of a localized bump of the form $h = \alpha\delta(\xi)$. In this case, integrating (3.1) through $\xi = 0$ one obtains $s^+ - s^- = -3\alpha$,

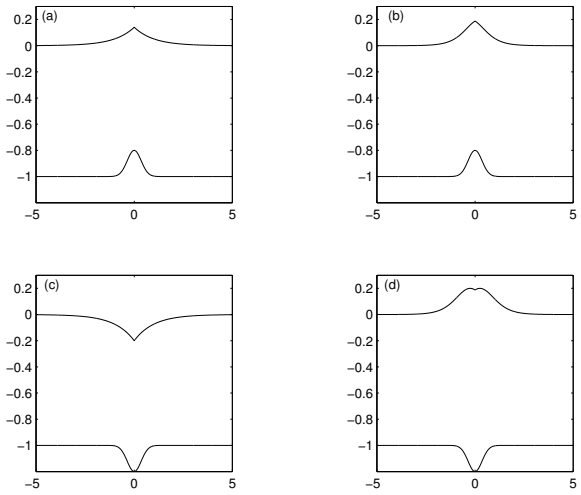

FIG. 3.3. *Sketches of various solutions obtained from Figure 3.2 for $E = 0$. (a) small amplitude wave over bump; (b) large amplitude wave over bump; (c) localized depression over hole; (d) dimpled wave over hole. Solutions with periodic waves ($E \neq 0$) can be found in [3]*

where

$$s^{\pm} = \lim_{\xi \to 0^{\pm}} \eta_x. \tag{3.6}$$

Thus the free surface has a corner over the extremum of the topography. A positive bump ($\alpha > 0$) corresponds to a negative jump in the slope of the free surface, and, conversely, a depression on the bottom gives a positive jump in the free surface slope.

For $f > 0$, we show in Figure 3.2 how to construct steady bounded solutions with mean zero and the appropriate jump in s over the bump. Solutions shown include a vertical jump of size 3α connecting to the smooth solutions away from the bump.

For $\alpha < 0$ there is a simple solution where the free surface has a localized depression (see the $\eta < 0$ trajectory) with a corner at the trough (see Figure 3.3 (c)). This solution exists for *all* $\alpha < 0$. There are other more complicated solutions obtained by following the homoclinic orbit for more than half of its length and jumping *up* to either the upper branch of the orbit (yielding a wave of elevation with a dimple at the crest see Figure 3.3 (d)) or to a periodic solution (which would require $E \neq 0$). These more complicated steady configurations exist for $-\frac{8}{9}\sqrt{2}f^{3/2} < \alpha < 0$ but are not usually observed for the full problem.

For $\alpha > 0$ there are two $E = 0$ solutions, both with corners at the crest from the two possible equal jumps in η_x for $\eta > 0$ trajectories: a small amplitude solution (see Figure 3.3 (a)), and a large amplitude solution similar to the solitary wave (see Figure 3.3 (b)). These solutions exist *only* for $0 < \alpha < \frac{8}{9}\sqrt{2}f^{3/2}$. For larger bumps there are no steady solutions. Alternatively, for a fixed bump size there is a $f_{crit} > 0$ below which there is no steady solution and above which there are two steady solutions. The behavior is that of a saddle-node bifurcation as f is increased through f_{crit}. In addition to these, jumps with $0 < \alpha < \frac{8}{9}\sqrt{2}f^{3/2}$, may also connect to periodic solutions if $E \neq 0$.

For $f < 0$ there are no localized solutions satisfying $\eta \to 0$ since the $\eta = 0$ fixed point is now a center. Figure 3.4 however, shows the possibility of a steady horizontal

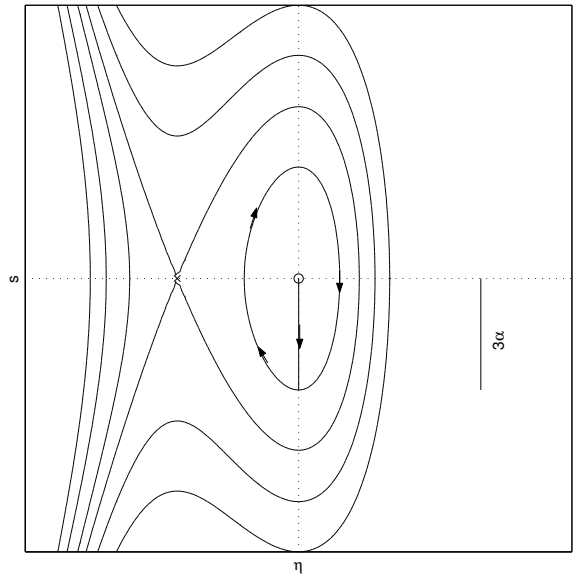

FIG. 3.4. *Solutions to the steady problem for $f < 0$ with Dirac topography $h = \alpha\delta(x)$. The free-surface has a jump in slope of -3α over the bump. The solution shown for $\alpha > 0$ connects an upstream flat free surface to periodic waves downstream. If the jump is sufficiently large then the solution is a hydraulic fall to a downstream horizontal free surface at the level of the saddle. The solutions for $\alpha < 0$ are similar.*

free surface on one side of the obstacle and a periodic wave on the other side. To understand whether these waves appear upstream or downstream, we consider an argument [5] based on a linearization of (2.15).

The behavior of the linear waves is obtained by substituting $\eta = \exp(ik\xi - \omega\tau)$ into the linearized and unforced (2.15) and obtaining

$$\omega = fk + \frac{1}{6}k^3, \qquad c_p = f + \frac{1}{6}k^2, \qquad c_g = f + \frac{1}{2}k^2. \tag{3.7}$$

Here ω is the frequency, k the wavenumber (inversely proportional to wavelength), and c_p, c_g, the phase and group velocity, respectively. For $f < 0$, steady waves of wavenumber

$$k = \sqrt{-6f} \tag{3.8}$$

(obtained at $c_p = 0$) are expected. These waves will form *downstream* from the obstacle since they propagate at the group speed and $c_g > 0$ for these waves.

These flat-periodic solutions, however, do not have mean zero and require a nonzero E. The effect of $E > 0$ on Figure 3.4 is to move the center to the right ($\eta > 0$ upstream) and the saddle to the left. However, E is a priori unknown, and therefore the simple arguments for the scaling between α and f valid for $f > 0$ do not apply. In the limiting case the solution can jump from the center $\eta > 0$ upstream to the homoclinic orbit, asymptoting to $\eta < 0$ downstream. We shall describe this as a "hydraulic fall" over the bump. Note that the solutions here are similar for $\alpha > 0$ and $\alpha < 0$.

There are several authors that have computed steady solutions, similar to those described above, to the full potential flow problem with a free surface. See, for

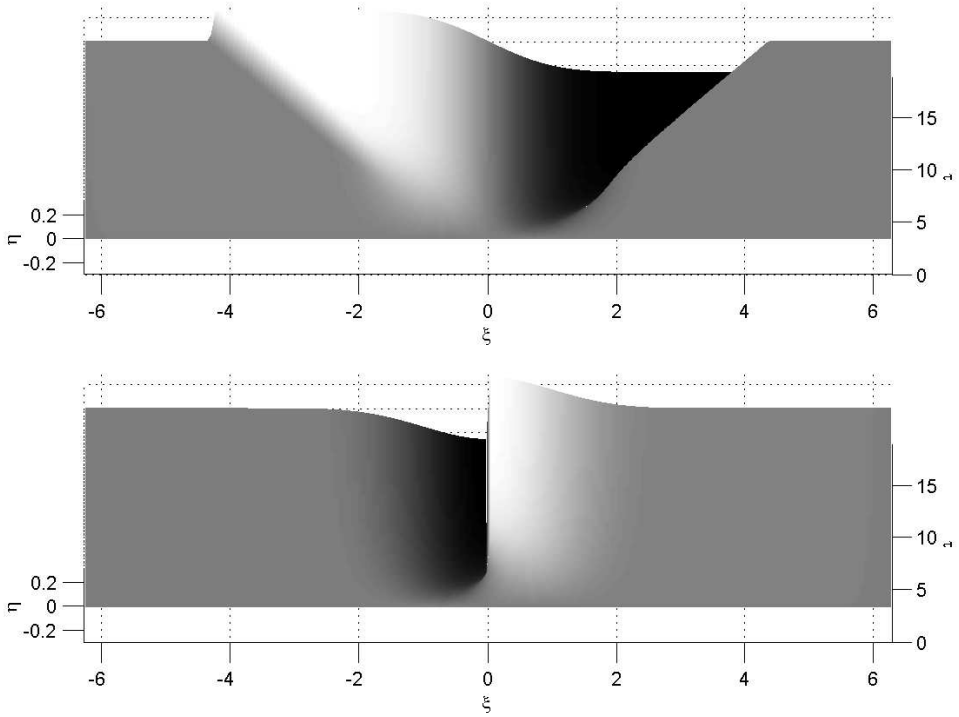

FIG. 4.1. *Free surface evolution of a flow over a bump according to the forced Burgers (4.1) equation for the case* $\frac{3}{2}\Delta h > f^2$ *(here* $f = 0$*,* $\Delta h = 0.1$*). Hydraulic fall over a bump (top) and a shock trapped in a hole (bottom). Flow is from left to right.*

example, [10]. The solutions obtained are qualitatively similar to those discussed here. Throughout the discussion of steady configurations, one must keep in mind that the solutions found may not be stable, and, therefore, may not be observed in time-dependent solutions.

4. Localized topography and time dependent solutions.

4.1. Hydraulic approximation. Another possible approximation of (2.15) is the hydraulic, or shallow water approximation [4]. In this case, we neglect the dispersive term and obtain

$$\eta_\tau + f\eta_\xi - \frac{3}{2}\eta\eta_\xi = \frac{1}{2}h_\xi(\xi). \tag{4.1}$$

Although our results here are independent of the precise shape of the bump we may think of h as a Gaussian: $h(x) = \alpha \exp(-\xi^2)$. This "forced" Burger's equation can be solved by the method of characteristics for $\xi(\tau, \xi_0)$ and $u(\tau, \xi_0)$

$$\frac{d\xi}{d\tau} = f - \frac{3}{2}u, \qquad \xi(0) = \xi_0, \tag{4.2}$$

$$\frac{du}{d\tau} = \frac{1}{2}h_\xi, \qquad u(0) = 0. \tag{4.3}$$

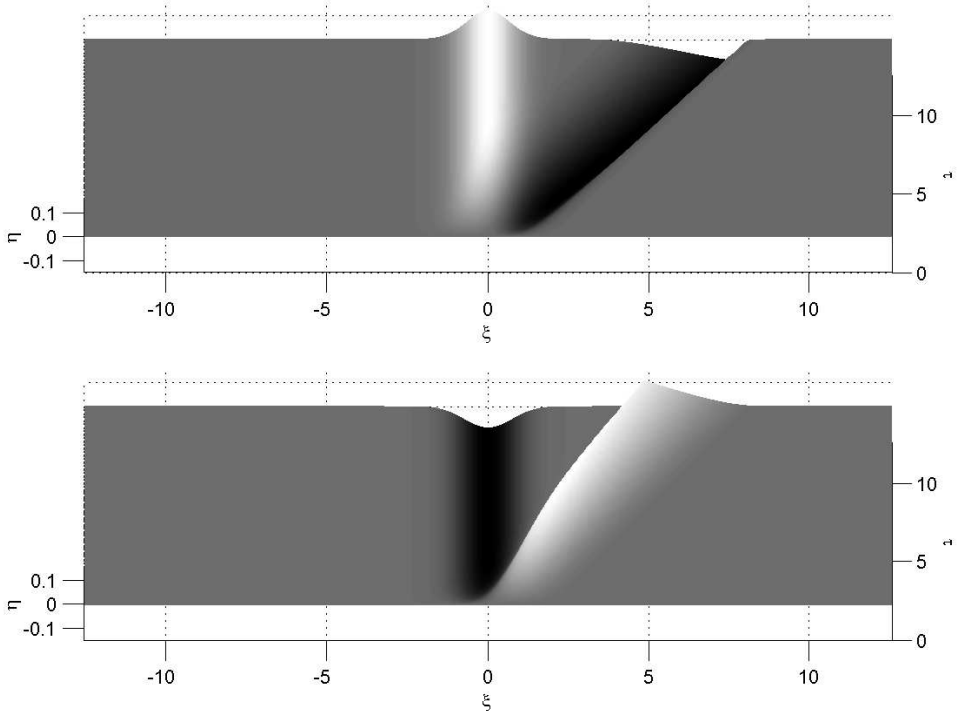

FIG. 4.2. *Free surface evolution of a flow over a bump according to the forced Burgers (4.1) equation for the case* $\frac{3}{2}\Delta h < f^2$ *(here* $f = 0.5$*,* $\Delta h = 0.1$*. Flow over a bump (top) and over a hole (bottom). Flow is from left to right.*

From these, one can obtain an equation for the characteristics

$$\frac{d\xi}{d\tau} = \pm f\left(1 - \frac{3}{2}\frac{h(\xi) - h_0}{f^2}\right)^{\frac{1}{2}}, \tag{4.4}$$

where $h_0 = h(\xi_0)$. The characteristics will change directions over the topography if $\frac{3}{2}\Delta h > f^2$, where Δh is the maximum height change of the topography. From (4.4) and (4.2) one obtains, for smooth parts,

$$u = \frac{2}{3} f\left(1 \mp \sqrt{1 - \frac{3}{2}\frac{h - h_0}{f^2}}\right) \tag{4.5}$$

When the characteristics turn, the sign in (4.4) changes, and $u = \frac{2}{3}f$. When characteristics intersect, a shock forms, and from (4.1) the shock speed s is

$$s = f - \frac{3}{4}(u_l + u_r), \tag{4.6}$$

where u_l, u_r are the left and right values of u at the shock. We discuss below the main cases that occur, and illustrate them with time-dependent calculations based on a Godunov scheme [6].

For a positive bump and $f > 0$, there will always be a shock forming downstream since characteristics starting over the bump will accelerate descending it and cross

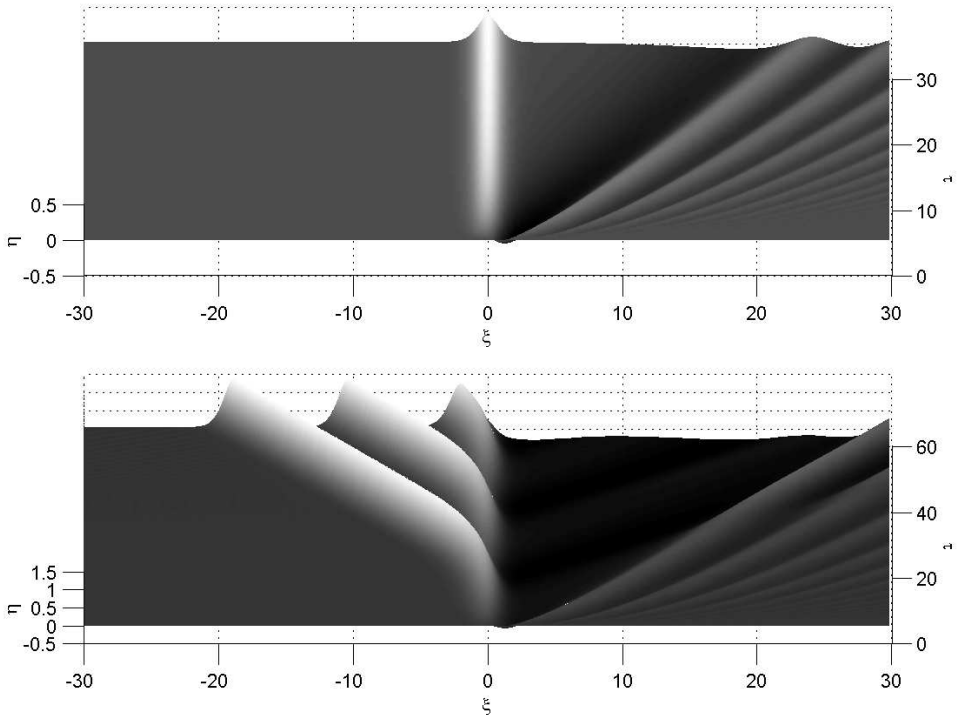

FIG. 4.3. *Free surface evolution of a supercritical flow over a bump according to the forced KdV (2.15) equation with* $h = \frac{1}{2}\sqrt{\frac{2}{\pi}}\exp\left(-\frac{x^2}{2}\right)$, *and* $f = 0.5$ *(top),* $f = 0.25$ *(bottom). Flow is from left to right.*

the characteristics from the flat part of the bottom. Since $u_l < 0$ and u_r is zero, for $f > 0$ this shock will be carried downstream.

If $\frac{3}{2}\Delta h > f^2$, upstream characteristics can not cross over the bump. Since they must turn around, there will be an upstream shock with $u_l = 0$, $u_r > 0$ and $s < 0$. Thus, after long times, and in the vicinity of the bump, the solution will be a hydraulic fall: a smooth transition between an elevated flat free surface upstream and a lower flat surface downstream (see Figure 4.1 top). If $\frac{3}{2}\Delta h < f^2$, upstream characteristics can travel over the bump and continue downstream. The downstream shock propagates away, thus leaving a steady localized elevation of the free surface over the bump (see Figure 4.2 top).

For a positive bump and $f < 0$, the solutions are similar to those above since the equation (4.1) is invariant under $f \to -f$, $u \to -u$, and $\xi \to -\xi$.

The solutions change considerably for a negative bump (hole). Here, for $f = 0$ the solution will form a shock which remains trapped in the hole (see Figure 4.1 bottom). For $f > 0$ a shock will form either in the hole or downstream of the hole and propagate downstream, leaving a localized depression in the free surface over the hole (see Figure 4.2 bottom). Similarly, the behavior for $f < 0$ can be obtained by the invariances of the equations. There is never a hydraulic fall in this case.

A complete characterization of solutions to the forced Burgers equation in a periodic domain can be found in [6].

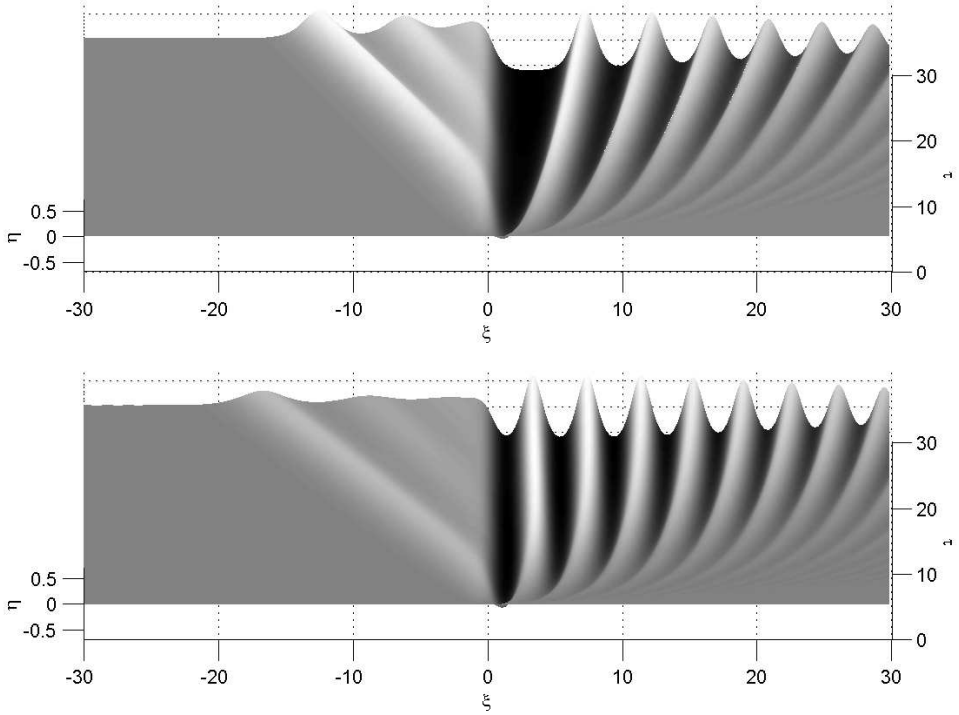

FIG. 4.4. *Free surface evolution of a subcritical flow over a bump according to the forced KdV (2.15) equation with* $h = \frac{1}{2}\sqrt{\frac{2}{\pi}}\exp\left(-\frac{x^2}{2}\right)$*, and* $f = -0.25$ *(top),* $f = -0.5$ *(bottom). Flow is from left to right.*

4.2. Time dependent Korteweg-de Vries solutions. With the understanding of steady forced KdV solutions and of the shallow water Burgers' limit, we now discuss typical time dependent solutions for the forced KdV equation. All solutions shown are computed using a pseudo-spectral numerical scheme [8]. The domain on which the solution was computed is periodic, however, only the neighborhood of the obstacle is shown. The initial data, for all cases, is zero.

We show first a sequence of distinct cases with a localized bump $h > 0$. The amplitude of the bump is fixed in the four pictures, but the Froude number f changes from strongly supercritical in Figure 4.3 (top) to strongly subcritical in Figure 4.4 (bottom). The flow is always from left to right.The four distinct cases are: **1**. Figure 4.3 (top): The flow is strong enough that all transients are swept downstream and the free surface in the vicinity of the bump is steady with an elevation over the bump. This steady solution near the bump is the smooth version of the case described in Figure 3.3 (a), and the wave transient carried downstream is an "undular bore": a wave connection between the two different free-surface levels on either side of the downstream shock in Figure 4.2 top. **2**. Figure 4.3 (bottom): The Froude number is now reduced so that there is no possible steady solution ($f < f_{crit}$ in Figure 3.2), and, in addition to the transient bore downstream there is a periodic generation of upstream waves. The upstream waves are free solitary waves of the KdV equation and are periodically shed when the free surface response over the bump becomes too large. This is a new, genuinely unsteady nonlinear phenomenon, not captured by

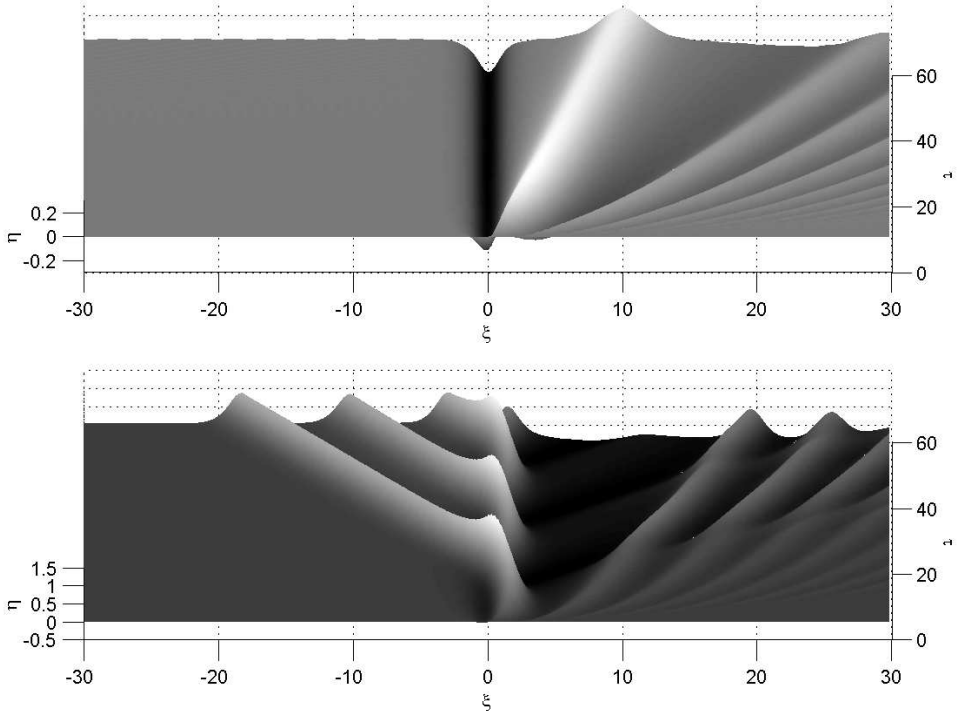

FIG. 4.5. *Free surface evolution of a supercritical flow over a hole according to the forced KdV (2.15) equation with* $h = -\frac{1}{2}\sqrt{\frac{2}{\pi}}\exp\left(-\frac{x^2}{2}\right)$, $f = 0.25$ *(top),* $f = 0$ *(bottom). Flow is from left to right.*

simpler models. There is also a net hydraulic fall over the obstacle as in Figure 4.1 top. **3**. Figure 4.4 (top): The flow is now slightly subcritical. There is a steady solution consisting of a "hydraulic fall" over the bump, as in Figure 4.1 top, and there are transient upstream and downstream undular bores. This case is related to Figure 3.4. **4**. Figure 4.4 (bottom): The flow is now strongly subcritical, and the steady solution corresponds to an upstream surface elevation with a downstream periodic wave train (also called lee waves) which is steady in the frame of the bump. This case is related to Figure 3.4.

Next, we consider a similar sequence for $h < 0$ (hole). **1**. Figure 4.5 (top): The flow is sufficiently strong that all transients are swept downstream and the free surface in the vicinity of the bump is a steady depression. This is a smooth version of the case described in Figure 3.3 (c). **2**. Figure 4.5 (bottom): The Froude number is now reduced and there is a periodic generation of upstream waves, and a hydraulic fall over the hole. The unsteady flow directly over the topography is more dramatic than in the bump case with large free surface variations. These probably arise from the hydraulic tendency to trap the shock. **3**. Figure 4.6 (top): The flow is now slightly subcritical, and the flow is similar to the previous case, but the waves are of smaller amplitude. The hydraulic fall over the bump can be predicted from Figure 3.4 for sufficiently large topography (α) relative to f. **4**. Figure 4.6 (bottom): The flow is now strongly subcritical, and there are steady lee waves which also can be explained from Figure 3.4 for smaller α relative to f.

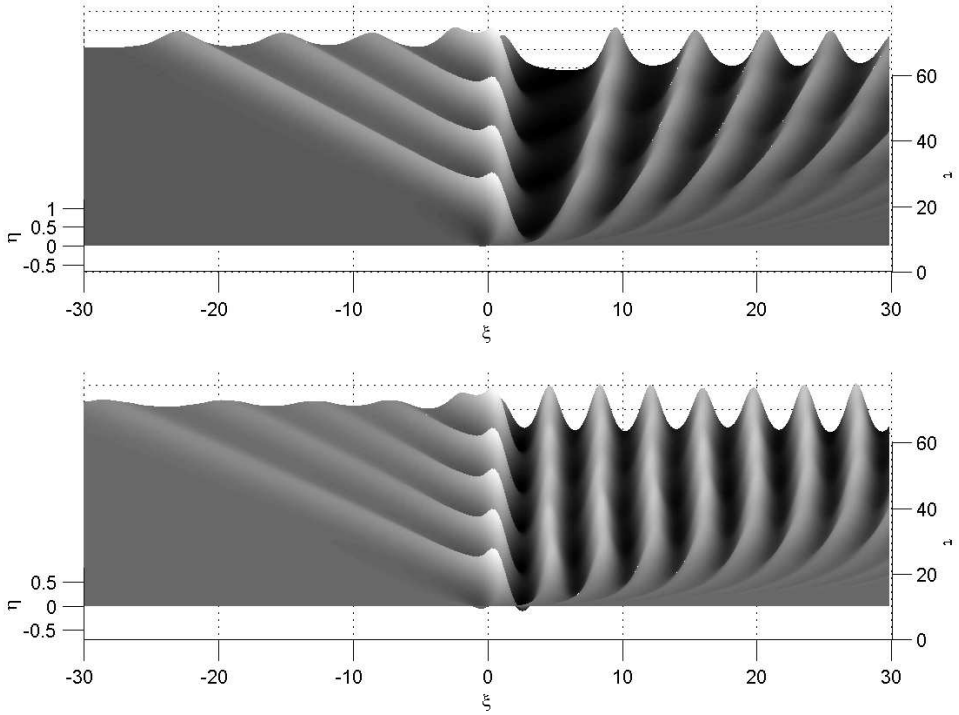

FIG. 4.6. *Free surface evolution of a subcritical flow over a hole according to the forced KdV (2.15) equation with* $h = -\frac{1}{2}\sqrt{\frac{2}{\pi}}\exp\left(-\frac{x^2}{2}\right)$, $f = -0.25$ *(top),* $f = -0.5$ *(bottom). Flow is from left to right.*

Solutions of the full time-dependent free-surface Navier-Stokes equations have also been computed for the flow over a bump [11]. There is qualitative agreement between those computations and those of KdV.

5. Extended topography. We now discuss some of the phenomena for extended topographical features such as plateaus ($\beta > 0$ below) and wide valleys ($\beta < 0$). Consider the topography given by $h = \beta\,[H(x+a) - H(x-a)]$, where $H(x)$ is the unit step function and $a \gg 1$. Then, seeking steady solutions, one would replace (3.1) by

$$f\eta - \frac{1}{6}\eta_{\xi\xi} - \frac{3}{4}\eta^2 = \frac{1}{2}\beta\,[H(\xi+a) - H(\xi-a)] - E. \tag{5.1}$$

Thus, at $\xi = \pm a$ the solutions and are continuous and have continuous derivatives, but have discontinuous second derivatives. They satisfy the equation with an additional constant term β for $-a < \xi < a$.

As an example, let us consider the subcritical case (where the steady problem has the phase plane as in Figure 3.1 (a)) of flow over a plateau ($\beta > 0$). If $E = 0$, over the plateau the fixed points move to $\eta = \frac{2}{3}\left(f \pm \sqrt{f^2 - 3\beta}\right)$. Thus a continuous solution starting upstream on the center at the origin in Figure 3.1 (a) will start a wave over the plateau since the new center will move to the left. This wave will have a negative mean surface elevation. Then, at the end of the plateau, the center moves back to the

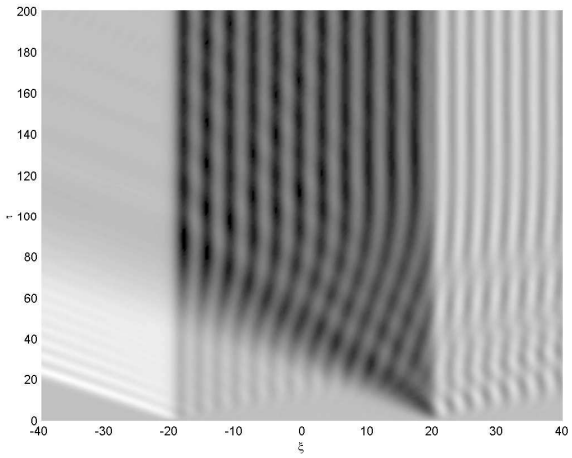

FIG. 5.1. *Grayscale plot of the free surface elevation of subcritical flow over a plateau situated at* $-20 < \xi < 20$. *In this calculation,* $\beta = 0.25$ *and* $f = -0.85$. *Flow is from left to right.*

origin, and the wave will continue as a trajectory about the origin. (It is possible to construct a steady solution with no waves downstream of the plateau for particular lengths of the plateau - a nonlinear eigenvalue problem - however these would not be physically relevant.) Figure 5.1 shows a subcritical flow's free surface elevation in the vicinity of a plateau and we see that the solution matches the description above. The wavelength over the plateau is longer than the wavelength downstream because the "effective" Froude number $(U/\sqrt{gH})$ over a plateau is larger and, from (3.8) this yields a longer wave. In numerical calculations we smoothen the step functions by using $1 + \frac{1}{2}\tanh(x)$.

If f is large one can argue that there is a steady free surface displacement with the same shape as the topography (and this is confirmed by computations), however for flows that are close to critical the behavior can be quite striking, especially in the case of a wide valley.

Figure 5.2 shows the time dependent evolution of flow over a valley. First, solitary upstream propagating waves are formed at the downstream wall of the valley. When they reach the upstream wall they either reflect back downstream or continue to propagate upstream away from the valley. Only sufficiently large waves can leave the valley upstream since they encounter an "effectively" larger Froude number as they exit the valley and therefore they must slow down. The reflected waves then appear to "perturb" the apparently unstable flow at the downstream wall and generate new upstream waves.

6. Conclusion. We have reviewed many aspects of a simple model for the free-surface flow over topography. Although the model is simple, it contains many of the phenomena of the full problem such as hydraulic falls, lee waves and upstream nonlinear wave propagation. For flows over a wide valley there are particularly striking transient flows with combinations of multiple reflections of trapped waves and escaping solitary waves. Some natural extensions to consider are the two-dimensional free surface case, and models for stratified fluid that allow for vertical propagation of wave energy.

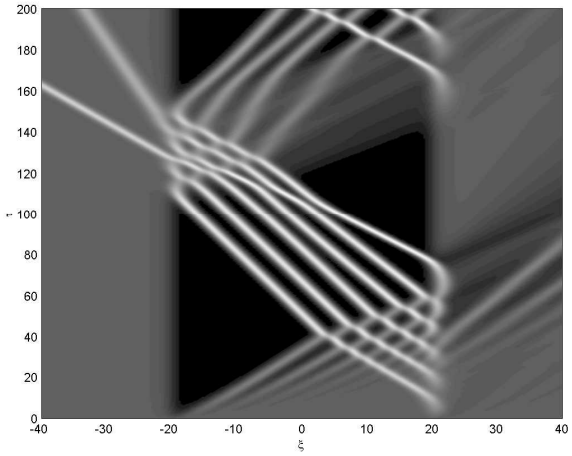

FIG. 5.2. *Grayscale plot of the free surface elevation of supercritical flow over a wide valley situated at* $-20 < \xi < 20$. *In this calculation,* $\beta = -0.25$ *and* $f = 0.25$. *Flow is from left to right.*

REFERENCES

[1] Baines, P., 1995: **Topographic effects in stratified flows**, *Cambridge University Press*

[2] Choi, J.; Milewski, P. A. Resonances between surface waves and periodic topography. To appear in *Studies in Appl. Math.* (2002)

[3] Dias, F.; Vanden-Broeck, J.-M. Two layer flows over an obstacle. To appear in *Phil. Trans. R. Soc. Lond. A* (2002).

[4] Grimshaw, R. H. J.; Smith, N., 1986 Resonant flow of a stratified fluid over topography. *J. Fluid Mech.* **169**, 429–464.

[5] Lighthill, J., 1978: **Waves in Fluids**, *Cambridge University Press*

[6] Menzaque, F.; Rosales, R. R.; Tabak, E. G.; Turner, C. V., 2001: The forced inviscid Burgers equation as a model for nonlinear interactions among dispersive waves. *Contemporary Mathematics* **283**, 51–82.

[7] Mielke, A., 1986: Steady flows of inviscid fluids under localized perturbations. *J. Diff. Eq.* **65**, 85–116.

[8] Milewski, P. A.; Tabak, E. G., 1999: A pseudo-spectral algorithm for the solution of nonlinear wave equations, *SIAM J. Sci. Comp.* **21**, 1102–1114.

[9] Milewski, P. A.; Vanden-Broeck, J.-M., 1999: Time-dependnt gravity-capillary flows past an obstacle, *Wave Motion* **29**, 63–79.

[10] Vanden-Broeck, J.-M., 1988: Free surface flow over a semi-circular obstruction in a channel, *Phys. Fluids* **30** 2315–2317.

[11] Nadiga, B. T.; Margolin, L. G.; Smolarkiewicz, P. K., 1996: Different approximations of shallow fluid flow over an obstacle, *Phys. Fluids* **8** 2066–2077.

[12] Wu, T. Y., 1987: Generation of upstream advancing solitons by moving disturbances, *J. Fluid. Mech.* **184** 75–99.